Turkish Journal of Electrical Engineering & Computer Sciences

http://journals.tubitak.gov.tr/elektrik/

Research Article

Turk J Elec Eng & Comp Sci
(2017) 25: 3994 – 4005

doi:10.3906/elk-1608-312

Low-frequency exposure analysis using electric and magnetic field measurements and predictions in the proximity of power transmission lines in urban areas

Hamza Feza CARLAK*, Şükrü ÖZEN, Süleyman BİLGİN
Department of Electrical & Electronics Engineering, Faculty of Engineering, Akdeniz University, Antalya, Turkey

Received: 29.08.2016 • **Accepted/Published Online:** 20.06.2017 • **Final Version:** 05.10.2017

Abstract: In recent years, increasing energy demand has resulted in more loading in power transmission lines and correspondingly more electric and magnetic field occurrence. In this paper, electric and magnetic field levels around high voltage power transmission lines are measured and then calculated analytically by simulating the realistic case. Moreover, the field levels around these power lines have been predicted using multilayer perceptron artificial neural network (ANN) and generalized regression neural network models. Typical 154 kV power transmission line facilities of Turkey have been studied. Electric and magnetic field levels in the proximity of power transmission lines have been predicted with ANN models with high accuracies. Particularly, the MLPNN algorithm predicts the electric and magnetic field intensities with very high precision. The aim of this research is to create a reference for researchers focused on topics of occupational and general public exposures and also biological effects of electric and magnetic fields emitted from low-frequency power transmission lines.

Key words: Power transmission lines, magnetic and electric field exposures, multilayer artificial neural networks, occupational and general public safety

1. Introduction

High voltage power line researchers have mostly focused on magnetic field exposure studies. Power frequency electric and magnetic fields have received important attention due to concerns that exposure to such fields might cause undesired health effects [1–6]. One of the recent studies showed that the leukemia risk for children and the cancer risk of adults have been increasing due to residential exposure to ELF-EMF. People who live in 50-m vicinity of transmission line have 33% higher cancer risk to people who live in the field of 50 m to 100 m [7–9]. The analytical and numerical studies of the electric field are less than the magnetic field studies. However, outdoor exposure to the electric fields around power transmission lines may have harmful effects and should be taken into account for human health.

Well-known environmental health organizations have determined limit values for magnetic field exposure levels. Most organizations accept 0.4 μT and a few of them 0.2 μT for long-term exposure as a critical leukemia level [8,10–12]. The level of 0.3–0.4 μT has been declared as a critical value for leukemia by the National Institute of Environmental Health Sciences and the International Agency for Research on Cancer (IARC, member of WHO) accept this limit value as the Group-B level [11–14]. The limit value recommended by the International Non-ionizing Radiation Committee (ICNIRP) for the public is 200 μT (2000 mG) [12], which is considerably higher than the other well-known authority health organizations. In residential life, childhood

*Correspondence: fezacarlak@akdeniz.edu.tr

cancers and occupational cancers such as breast and brain cancer and leukemia have been dramatically increasing due to the harmful effects of power frequency electromagnetic fields on human health. There are also other undesired detrimental effects of electromagnetic field exposure, i.e. the increase in the risk of miscarriage [15,16], neurodegenerative diseases such as amyotrophic lateral sclerosis, Alzheimer's disease [7], suicide mortalities [17], and susceptibility to depressive illness and to myocardial infarctions [18].

In recent years, artificial neural network techniques have been effectively used to predict the electromagnetic fields in overhead power transmission lines [19–22]. This study will shed light on the comparison of traditional methods with artificial neural network methods to estimate the electric and magnetic fields around power transmission lines. For this goal, electric and magnetic field variations around typical power lines are investigated. Analytical and numerical methods for the calculation of electric and magnetic fields around power transmission and distribution lines are implemented.

In this study, residential electric and magnetic fields radiated from typical high voltage power lines are measured, and then the prediction of magnetic and electric fields around the typical power transmission lines is performed with respect to the measurement data and compared with measurement and analytical results. Artificial neural network algorithms, namely multilayer perceptron neural networks (MLPNNs) and generalized regression neural networks (GRNNs), are investigated as an alternative approach to predict magnetic and electric field levels.

2. Electric and magnetic field measurements

Residential electric fields radiated from typical high voltage power lines in Turkey are measured by using a CA42 LF field meter, which is made by Chauvin Arnoux. Electric field measurements are taken at 1-m height from ground level, and the coordinates of the 154 kV power lines are given in Table 1. Since 154-kV power lines pass through urban areas in Turkey, measurements are acquired particularly for this voltage level. The instantaneous current value of the transmission line is recorded about 156.3 A in the measurement period. Magnetic field strengths emitted by 154-kV typical high voltage power lines in Turkey are measured by using the Magnetic Field Hitester 3470 with the magnetic field sensor 3471. Measurements are taken at different heights from ground level. The location and coordinates of the 154-kV power transmission line are denoted in Table 1. The data of the electric and magnetic field measurements are expressed in Tables 2 and 3.

Table 1. Coordinates of the power transmission line conductors.

Coordinates	Phase R	Phase S	Phase T
x (m)	-6.6	0.0	6.6
y (m)	17.5	17.5	17.5

2.1. Analytical calculation of electric and magnetic fields

The electric and magnetic fields are determined by the prediction methods and measurements. In this study, the charge simulation method (CSM) is implemented to obtain the electric fields around the high voltage transmission lines and the Biot–Savart rule is used to calculate the magnetic field by using time-dependent current [23]. For a long-term prediction, load characteristics of the lines are considered for a year period. In the literature, there are a limited number of studies on electric and magnetic field exposure analysis using multilayer artificial neural network algorithms, which present an alternative approach beside traditional methods.

Table 2. Electric field measurement data.

X-Coordinates (m)	Y-Coordinates (Height)				
	0.2 m	0.5 m	1 m	1.5 m	2 m
	$E_{measured}$ (kV/m)				
0	1.124	1.160	1.224	1.294	1.369
2	1.109	1.144	1.207	1.275	1.348
4	1.079	1.113	1.173	1.238	1.308
6	1.036	1.068	1.123	1.183	1.248
8	0.972	1.000	1.049	1.102	1.159
10	0.902	0.926	0.969	1.015	1.064
12	0.826	0.847	0.883	0.921	0.961
14	0749	0.766	0.796	0.827	0.860
16	0.675	0.689	0.713	0.738	0.764
18	0.604	0.615	0.634	0.653	0.674
20	0.542	0.551	0.566	0.581	0.598
22	0.485	0.492	0.504	0.516	0.529
24	0.432	0.438	0.447	0.457	0.467
26	0.389	0.394	0.401	0.409	0.417
28	0.350	0.354	0.360	0.366	0.372
30	0.315	0.317	0.322	0.327	0.332
32	0.286	0.288	0.292	0.296	0.300
34	0.259	0.261	0.264	0.268	0.271
36	0.235	0.237	0.240	0.242	0.245
38	0.215	0.217	0.219	0.221	0.223
40	0.197	0.199	0.200	0.202	0.204

2.2. Prediction of electric and magnetic fields with artificial neural network algorithms

2.2.1. Multilayer perceptron neural networks (MLPNNs)

The MLPNN method is used as one of the most common neural network algorithms and it may include two or more layers as shown in Figure 1. The number of input layer neurons is equal to the number of selected specific features and the output layer determines the desired output classes, which decide the number of neurons in the output layer. The hidden layers between the input and output layers may be used for optimizing the MLPNN method especially for nonlinear systems. The most common method of finding the optimum number of neurons and hidden layers is using the process of trial-and-error [24].

For one perceptron, the MLPNN is shown as

$$x = \sum_{i=1}^{R} w_i p_i + b, \tag{1}$$

where R is the number of inputs and their weights, p_i is the input value of a perceptron, $w_i w_i$ is the weight for each input, and x is the summation of a perceptron. The summation of the perceptron is scaled with a tangent sigmoid activation function (in hidden layers) and linear transfer function (in the output layer). The output y of a perceptron for the tangent sigmoid function in the hidden layers is denoted as

$$y = f(x) = \frac{e^x - e^{-x}}{e^x + e^{-x}} \tag{2}$$

Table 3. Magnetic field measurement data.

X-Coordinates (m)	Y-Coordinates (Height)				
	0.2 m	0.5 m	1 m	1.5 m	2 m
	$H_{measured}$ (μT)				
0	1.532	1.590	1.649	1.760	1.850
2	1.512	1.578	1.630	1.710	1.810
4	1.458	1.530	1.610	1.700	1.800
6	1.389	1.465	1.500	1.590	1.720
8	1.324	1.378	1.410	1.480	1.600
10	1.225	1.260	1.320	1.390	1.480
12	1.125	1.140	1.270	1.280	1.300
14	1.010	1.023	1.070	1.100	1.200
16	0.962	0.980	0.990	0.960	1.000
18	0.851	0.820	0.850	0.890	0.950
20	0.731	0.740	0.745	0.820	0.770
22	0.654	0.680	0.670	0.680	0.680
24	0.572	0.579	0.580	0.600	0.620
26	0.514	0.520	0.530	0.540	0.530
28	0.473	0.500	0.469	0.470	0.470
30	0.412	0.430	0.410	0.450	0.400
32	0.382	0.369	0.375	0.400	0.380
34	0.321	0.356	0.340	0.367	0.340
36	0.301	0.300	0.297	0.280	0.300
38	0.280	0.290	0.270	0.282	0.280
40	0.261	0.245	0.245	0.290	0.260

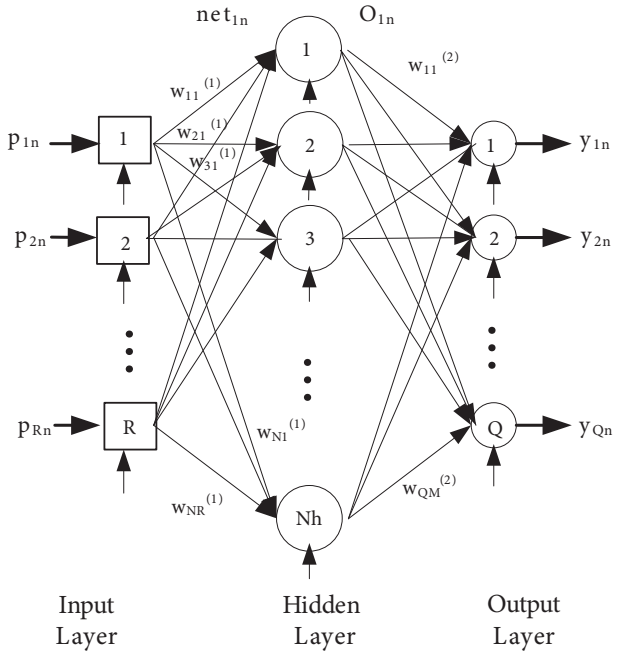

Figure 1. The structure of the MLPNN model.

Linear transfer function $y = f(x) = x$ can be calculated at the one perceptron in the output layer. The

structure of the MLPNN model is shown in Figure 1. $\{(p_n, t_n)\}$ are training patterns, n is the pattern number, R and Q are the dimensions of the input vector p_n and the desired output vector t_n, respectively, and vector y_n is the network output of the n-th pattern. For the I-th hidden unit, the net input $net_n(I)$ and the output activation $O_n(I)$ for the n-th training pattern are

$$net_n(i) = \sum_{j=1}^{R+1} \omega(i,j).p_n(j), \quad 1 \le i \le N \tag{3}$$

$$O_n(i) = f(net_n(i)), \tag{4}$$

where $\omega(I,j)$ shows the weight connecting the $j-$th input unit to the $I-$th hidden unit. The $k-$th output for the $n-$th training pattern is y_{nk}, given as the following equation:

$$y_{nk} = \sum_{j=0}^{R+1} \omega_{jo}(k,j) \cdot p_n(j) + \sum_{i=1}^{Nh} \omega_{ho}(k,i) \cdot O_n(i), 1 \le k \le Q, \tag{5}$$

where $\omega_{io}(k,j)$ denotes the output weight connecting the $j-$th input unit to the $k-$th output unit and $w_{ho}(k,I)$ denotes the output weight connecting the $I-$th hidden unit to the $k-$th output unit. The mapping error for the $n-$th pattern is given by

$$E_n = \sum_{k=1}^{Q} [t_{nk} - y_{nk}]^2, \tag{6}$$

where t_{nk} denotes the $k-$th element of the $n-$th desired output vector. Training a neural network in batch mode, the mapping error for the $k-$th output unit is formulized by

$$E(k) = \frac{1}{N_h} \sum_{n=1}^{N_h} [t_{nk} - y_{nk}]^2 \tag{7}$$

The overall performance of an MLPNN can be determined by evaluating the mean square error (mse) function, which can be given as

$$E = \sum_{k=1}^{Q} E(k) \tag{8}$$

2.2.2. Generalized regression neural networks (GRNNs)

The GRNN comprises four layers: input layer, pattern layer, summation layer, and output layer (see Figure 2). This regression tool consists of a dynamic network structure [25]. The GRNN model includes vectors that have X input values and Y output values. Thus, x and y are measured as values of X and Y, respectively, and $\hat{f}(x,y)$ is the joint continuous probability density function of X and Y. The joint probability density in the GRNN can be expressed as

$$\hat{f}(x,y) = \frac{1}{(2\pi)^{(d+1)/2}} \times \frac{1}{n} \sum \left[\exp\left(\frac{(x-x_i)^T (x-x_i)}{2\sigma^2} \right) \exp\left(\frac{(y-y_i)^2}{2\sigma^2} \right) \right], \tag{9}$$

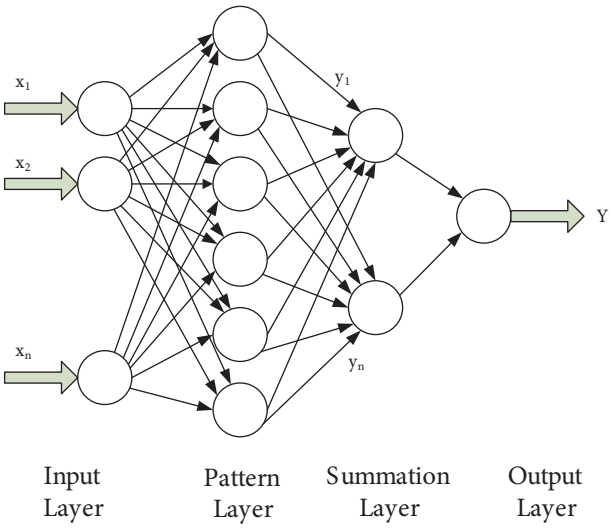

Figure 2. The structure of the GRNN.

where n is the sample observations, σ is the spread parameter, x_i is the 2-th training vector, and vector y_i is the corresponding value. The regression of Y on x can be formulated as

$$E\left[Y|x\right] = \frac{\int_{-\infty}^{\infty} Y.f(x,Y)dY}{\int_{-\infty}^{\infty} f(x,Y)dY} \tag{10}$$

and

$$\hat{y}\left(x\right) = E\left[Y|x\right] = \frac{\sum_{i=1}^{n}\left[y_i \exp(\frac{-d_i^2}{2\sigma^2})\right]}{\sum_{i=1}^{n}\exp(\frac{-d_i^2}{2\sigma^2})}, \tag{11}$$

where d_i is the distance between the input vector and the i-th training vector, which can be formulated as

$$d_i^2 = (x - x_i)^T (x - x_i) \tag{12}$$

The estimate $\hat{y}(x)$ is a weighted average of all observed y_i values.

3. Results

An MLPNN algorithm is implemented for the electric and magnetic field predictions. Neural network study is performed by applying the following procedures.

1. The normalization of the input and output dataset is implemented with maximum–minimum mapping ranging between –1 and 1. Input values are selected as the horizontal and vertical distance values. Electric field measurement values are inserted as the output values. The ANN structure has two input values and one output value.

2. Three-fold cross validation is implemented for the electric and magnetic field dataset. The database is divided into 66.67% train and 33.33% test data randomly.

3. The determination of target values is performed according to maximum–minimum mapping.

4. The MLPNN structure comprises an input layer including two neurons and three hidden layers. While the first and third layers have two neurons, the second layer has three neurons, which have a tangent sigmoid transfer function. The output layer has a single neuron, which has a linear transfer function.
5. The structure is determined experimentally and this structure achieves the highest score.
6. The structure is trained using the Levenberg–Marquardt algorithm that determines the optimum training results between other back propagation training algorithms used as an experimental comparison.
7. Test accuracy of training and testing simulations is determined according to mse scores.
8. The success of this method is compared with the other methods with regard to mse scores.

The second method used in electric and magnetic field predictions is the GRNN method. Three-fold cross validation is also implemented for the GRNN algorithm. The database comprises 66.67% train data and 33.33% test data. It has an input layer with two neurons, one pattern layer including radial basis functions, a summation layer, and an output layer including a single neuron. Spread factor, which is the only adjustable parameter of GRNN structure, is selected as 0.5 for this study. The spread parameter is the distance of an input vector from the weight vector of a neuron.

The MLPNN method has the best accuracy results (Table 4). The mse of the MLPNN algorithm is obtained as 0.000952051 for electric field and 0.00073935 for magnetic field studies. On the other hand, the GRNN algorithm has 0.002818 mse for the electric field and 0.001344 mse for the magnetic field with respect to the measurement database. The comparison of MLPNN and GRNN methods and analytical and measurement results of the electric and magnetic field are depicted in Figures 3 and 4. The results of the MLPNN algorithm match almost perfectly the measured data (see Figures 3 and 4). According to the mse analysis with respect to the measured values, the best results are obtained using the MLPNN algorithm. Numerical mse results are shown in Table 4.

Table 4. Mean square error values for the proposed methods.

MSE	MLPNN	GRNN
EF	0.000952051	0.002818
HF	0.00073935	0.001344

Analytical results of electric field intensities at different heights are denoted in Figure 5, and Figure 6 depicts the magnetic field intensities with respect to different coordinates. These results are obtained using MLPNN and GRNN methods.

To make a comparison and see the accuracy and precision, measured values are also denoted in Figures 7 and 8. The other method allows one to alter just one parameter. However, MLPNN allows one to change more parameters, which are neuron numbers, layer numbers, activation function types, etc. Therefore, the most accurate result can be obtained by the MLPNN algorithm.

The prediction of electric and magnetic field intensities at different heights and corresponding coordinates around power transmission lines are denoted in Figures 9 and 10. Results are obtained very precisely by using the MLPNN algorithm (see Figures 9 and 10). Figures 3 and 4 depict the accuracy of the neural network algorithms. In Figures 5–10, electric and magnetic field intensity values are shown with respect to horizontal and vertical locations. In Figures 5 and 6, analytical calculations are denoted, measured values are found in Figures 7 and 8, and MLPNN results are depicted in Figures 9 and 10. The results of measurement, theoretical (analytical calculation), and prediction algorithms are obtained in a consistent manner.

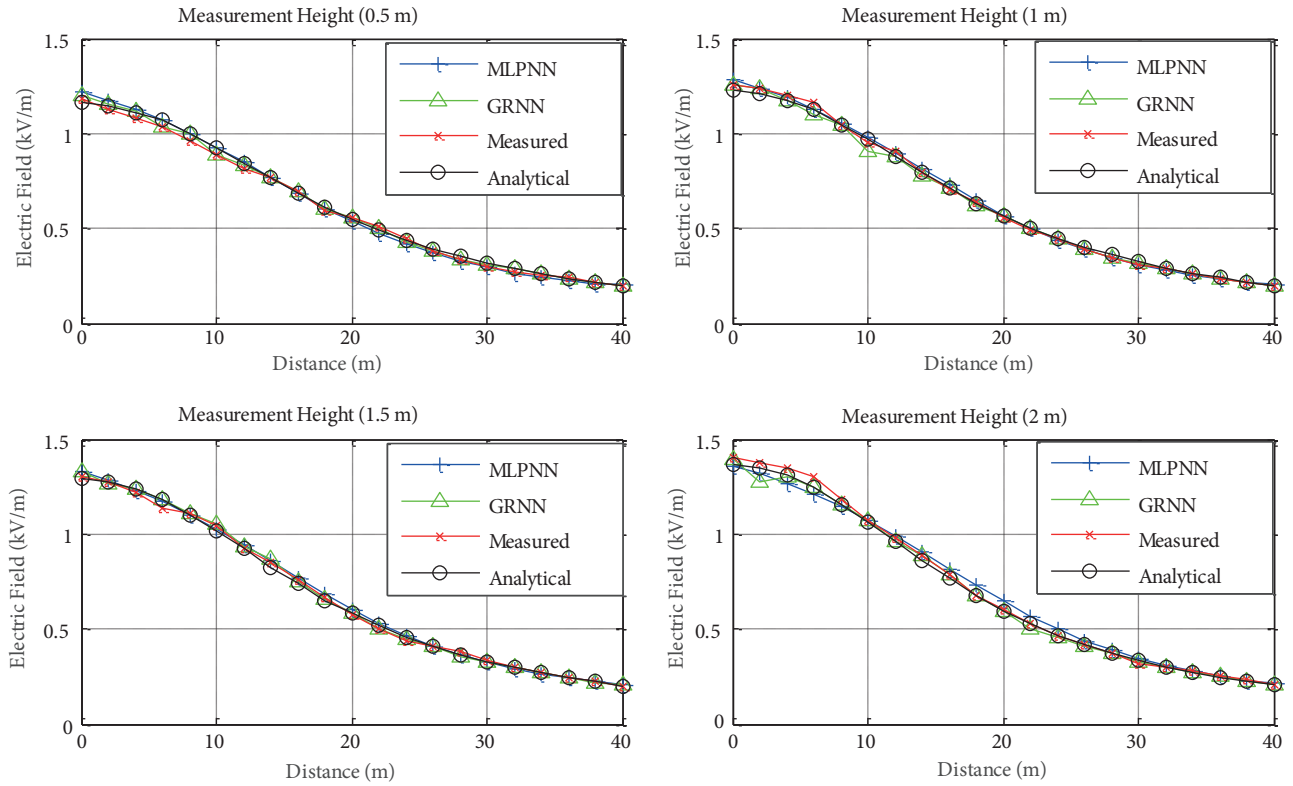

Figure 3. Electric field intensities at different heights. The results are obtained by measurement, analytical calculation, and artificial neural network algorithms (MLPNN and GRNN methods).

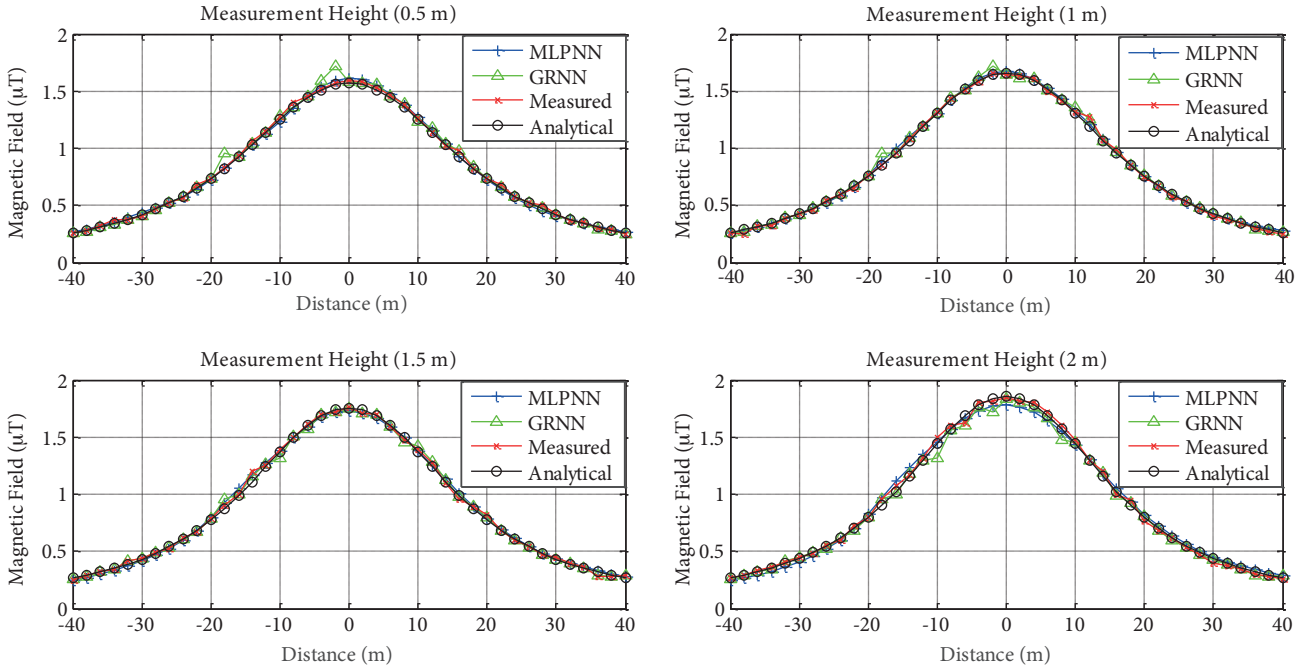

Figure 4. Magnetic field intensities at different heights. The results are obtained by measurement, analytical calculation, and artificial neural network algorithms (MLPNN and GRNN methods). The critical magnetic field exposure value (0.3–0.4 μT) is exceeded in 40-m proximity of the power-transmission line.

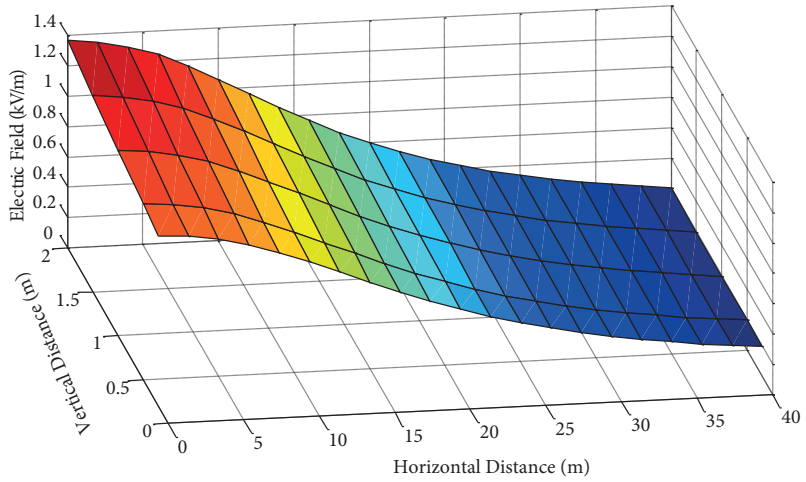

Figure 5. Electric field intensities with respect to horizontal and vertical coordinates. Electric field intensity values are obtained by analytical calculation.

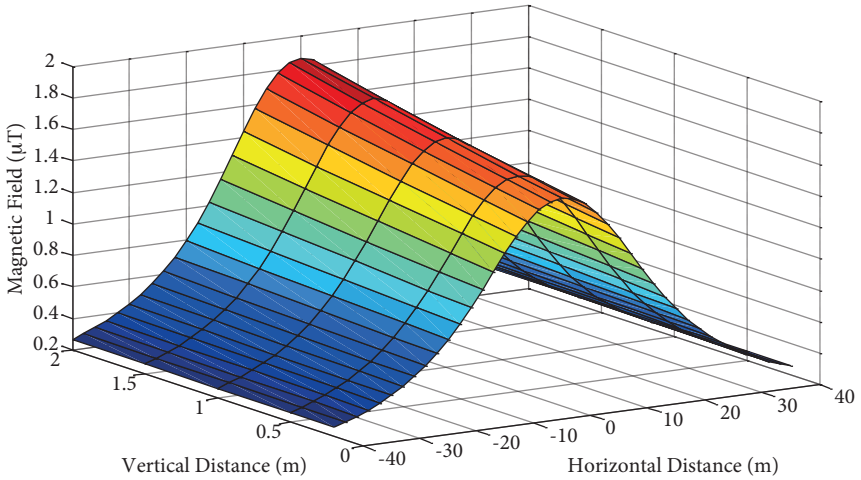

Figure 6. Magnetic field intensities with respect to horizontal and vertical coordinates. Magnetic field intensity values are obtained by analytical calculation.

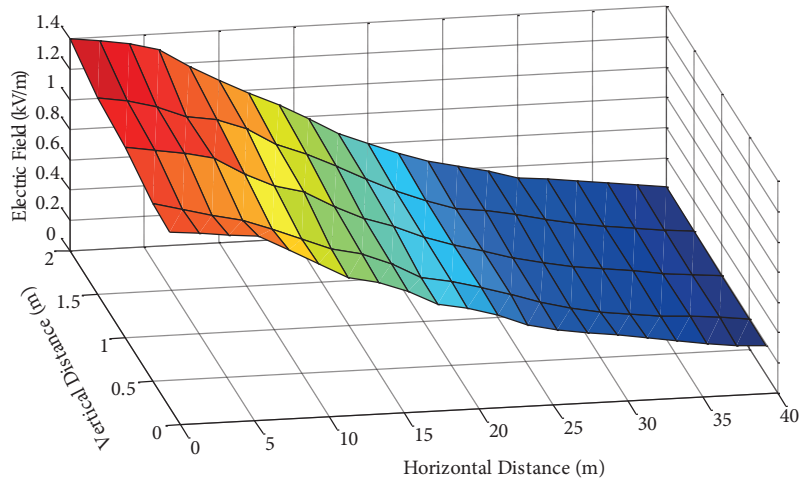

Figure 7. Electric field measurement values with respect to horizontal and vertical coordinates. Measurements are obtained from typical high-voltage power lines in Turkey.

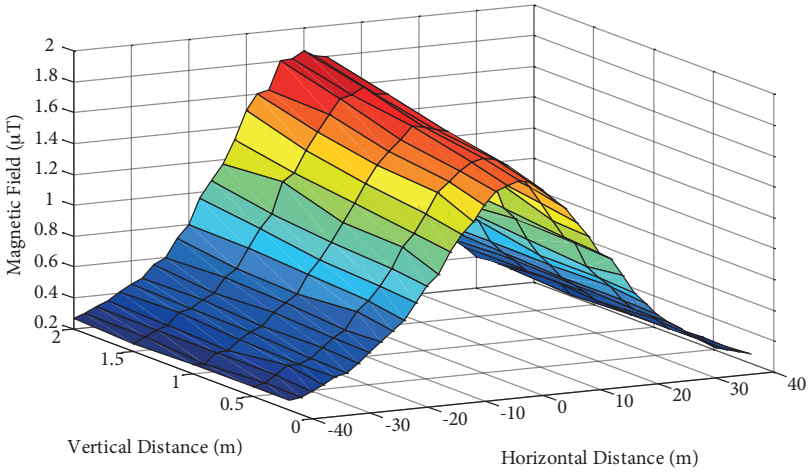

Figure 8. Magnetic field measurement values with respect to horizontal and vertical coordinates. Measurements are obtained from typical high-voltage power lines in Turkey.

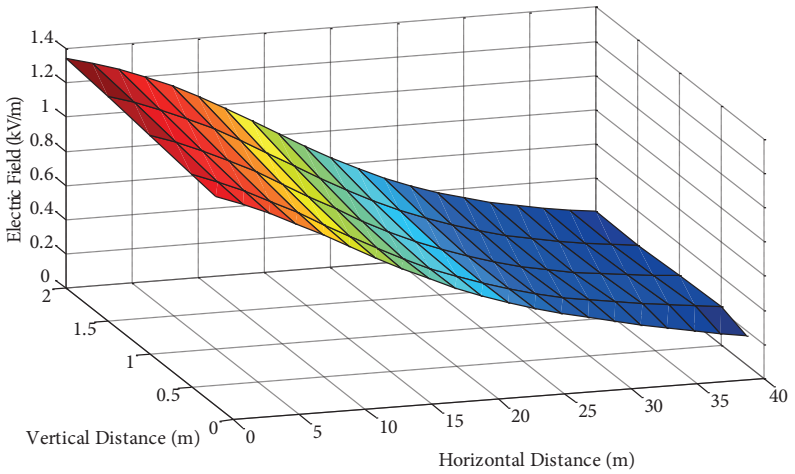

Figure 9. Electric field intensities with respect to horizontal and vertical coordinates. The MLPNN algorithm is performed to obtain electric field intensity values.

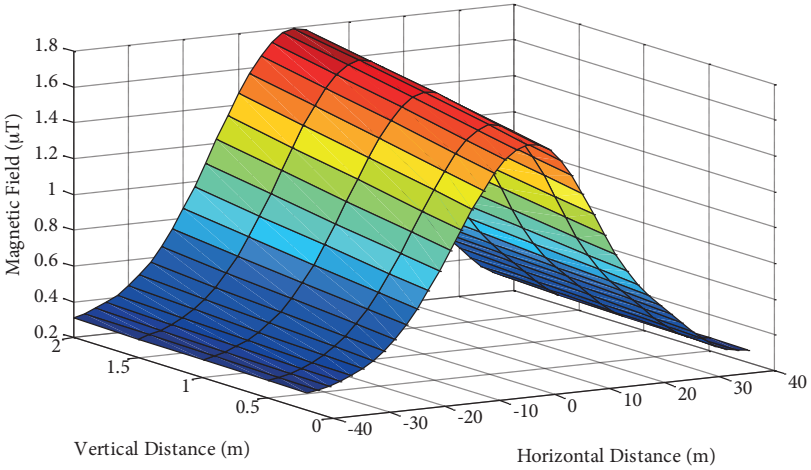

Figure 10. Magnetic field intensities with respect to horizontal and vertical coordinates. The MLPNN algorithm is performed to obtain magnetic field intensity values.

4. Conclusions

The studies on environmental and health effects of electric and magnetic field exposure have dramatically increased due to the increasing energy demand and requirement. Especially to perform risk analysis of the electric and magnetic field occurrences around the transmission lines passing through the urban areas, prediction methods are required.

In this study, ANN methods, namely multilayer perceptron neural networks (MLPNNs) and generalized radial basis neural networks (GRNNs), are compared with the measurement and analytical results to evaluate the success of neural network algorithms for the determination of electric and magnetic field intensities around the low-frequency power transmission lines. The MLPNN method has the best accuracy results.

The mse of the MLPNN algorithm is acquired as 9.52051×10^{-4} for the electric field and 7.3935×10^{-4} for the magnetic field with respect to the measurement database. The error values of the MLPNN algorithm are very low compared to the GRNN method. Three-fold cross-validation is also performed to demonstrate the accuracy of the Neural Network results. Cross-validation reveals the accuracy of the neural network algorithms with different combinations of train and test data and determines how realistic they are. Thereby, the reproducing situations of ANN structures are minimized. Numerical analysis denotes that the MLPNN algorithm is the best neural network method for the prediction of electric and magnetic field intensities. The prediction of the electric and magnetic field intensities can be implemented with very low error by neural network algorithms, especially the MLPNN method, by defining the line voltage level and the physical properties of the line.

The results reveal that magnetic field exposure limits are exceeded in 40-m vicinity of the 154-kV typical high voltage power lines in urban areas. Since the injected current values increase with the power demand, these electric and magnetic field exposure levels will also improve, and exposure to these fields will take place in wider areas. Therefore, electromagnetic field safety corridors should be set up for power transmission lines passing through urban areas. The results of this study indicate that neural network algorithms, particularly MLPNNs, can be used as a complementary tool with the conventional methods for the prediction of electric and magnetic field intensities around low-frequency power transmission lines for the study of bioelectromagnetic, occupational health and safety, electromagnetic risk analysis, and determination of the electromagnetic safety corridors for power transmission lines. To keep the general public and occupational exposure under control safely, electromagnetic field analysis of power transmission lines should be seriously implemented periodically for existing power transmission lines and the designs of new electric power line projects. Moreover, the prediction of the current densities induced in the bodies of electrical workers and people living in the vicinity of power lines might be implemented with the proposed ANN algorithms. Such a study would be beneficial in providing data for epidemiological studies to be carried out in this area.

Acknowledgment

The research is supported by the Research Project Department of Akdeniz University, Antalya, Turkey.

References

[1] Dennis JA, Muirhead CR, Ennis JR. Epidemiological studies of exposures to electromagnetic fields: I. General health and birth outcome. J Radiol Prot 1991; 11: 3-12.

[2] Stather JW. Epidemiological studies concerned with exposure to extremely low frequency electromagnetic fields and the risk of cancer. Radiat Prot Dosimetry 1997; 72: 291-303.

[3] Sahl JD, Kelsh MA, Greenland S. Cohort and nested case-control studies of hematopoietic cancers and brain cancer among electric utility workers. Epidemiology 1993; 4: 104-114.

[4] Draper G, Vincent T, Kroll ME, Swanson J. Childhood cancer in relation to distance from high voltage power lines in England and Wales: a case-control study. BMJ 2005: 330: 1-5.

[5] Gurney JG, Davis S, Schwartz SM, Mueller BA. Childhood cancer occurrence in relation to power line configurations: a study of potential selection bias in case-control studies. Epidemiology 1995; 6: 31-35.

[6] Ozen S. Low-frequency transient electric and magnetic fields coupling to child body. Radiat Prot Dosimetry 2008; 128: 62-67.

[7] Ahlbom IC, Cardis E, Green A, Linet M. Review of the epidemiologic literature on EMF and health. Environ. Health Perspect 2001; 109: 911-933.

[8] Coleman MP, Bell CM, Taylor HL. Leukemia and residence near electrical transmission lines: a case control study. Br J Cancer 1989; 60: 793-798.

[9] Deford JF, Gandhi OP. Impedance method to calculate currents induced in biological bodies exposed to quasi-static electromagnetic fields. IEEE T Electromagn C 1985; 27: 168-173.

[10] Abd-Allah MA, Mahmoud SA, Anis HI. Interaction of environmental ELF electromagnetic fields with living bodies. Electr Mach Pow Syst 2000; 28: 301-312.

[11] Ahlbom A, Day N, Feychting M, Roman E, Skinner J, Dockerty J, Linet M, McBride M, Michaelis J, Olsen JH et al. A pooled analysis of magnetic fields and childhood leukemia. Br J Cancer 2000; 83: 692-698.

[12] ICNIRP. Guidelines for limiting exposure to time-varying electric, magnetic, and electromagnetic fields up to 300 GHz. Health Phys 1998; 41: 449-522.

[13] Helhel S, Ozen S. Assessment of occupational exposure to magnetic fields in the high voltage substations (154/34.5kV). Radiat Prot Dosimetry 2008; 128: 464-470.

[14] Noble D, McKinlay A, Repacholi M. Effects of static magnetic fields relevant to human health. Prog Biophys Mol Bio 2005; 87: 171-372.

[15] IARC. Monographs on the evaluation of carcinogenic risks to humans, Non-ionizing radiation, Part 1: Static and extremely low-frequency (ELF) electric and magnetic fields. Lyon, France: International Agency for Research on Cancer 2002; Monograph, 80.

[16] Li DK, Odouli R, Wi S, Janevic T, Golditch I, Bracken TD, Senior R, Rankin R, Iriye R. A population-based perspective cohort study of personal exposure to magnetic fields during pregnancy and the risk of miscarriage. Epidemiology 2002; 13: 9-20.

[17] Wijngaarden VE, Savitz DA, Kleckner RC, Cai J, Loomis D. Exposure to electromagnetic fields and suicide among electric utility workers: a nested case-control study. Occup Environ Med 2000; 57: 258-263.

[18] Perry S, Pearl L, Binns R. Power frequency magnetic field; depressive illness and myocardial infarction. Public Health 1989; 103: 177-80.

[19] Charalambos PN, Antonis PP, Panos AR, George AK, John NS. Measurements and predictions of electric and magnetic fields from power lines. Electr Pow Syst Res 2011; 81: 1107-1116.

[20] Vesna R, Jasna R. Prediction of magnetic field near power lines by normalized radial basis function network. Adv Eng Softw 2011; 42: 934-938.

[21] Munoz F, Aguado JA, Martin F, Lopez JJ, Rodriguez A, Garcia JB, Treitero AR, Molina R. An intelligent computing technique to estimate the magnetic field generated by overhead transmission lines using a hybrid GA-Sx algorithm. Int J Elec Power 2013; 53: 43-53.

[22] Sivakami P, Subburaj P. EMF Estimation of over head transmission line using CS algorithm with aid of NFC. International Journal on Electrical Engineering and Informatics 2016; 8: 625-644.

[23] Ozen S, Ogel EG, Helhel S. Residential Area Medium Voltage Power Lines; Public Health, and Electric and Magnetic Field Levels. Gazi University Journal of Science 2013; 26: 573-578.

[24] Rumelhart DE, Hinton GE, Williams RJ. Learning representations by back propagating errors. Nature 1986; 323: 533-536.

[25] Specht D. A general regression neural network. IEEE T Neural Networ 1991; 2: 568-576.